Stability and equation of state of a nanocrystalline Ga-Ge mullite in a vitroceramic composite: A synchrotron x-ray diffraction study

Kristina E. Lipinska-Kalita,[1] Patricia E. Kalita,[2] Cédric Gobin,[2] Oliver A. Hemmers,[1]
Thomas Hartmann,[3] and Gino Mariotto[4]
[1]*Department of Chemistry, University of Nevada Las Vegas, 4505 Maryland Parkway, Box 454003, Las Vegas, Nevada 89154-4003, USA*
[2]*Department of Physics, University of Nevada Las Vegas, 4505 Maryland Parkway, Box 4002, Las Vegas, Nevada 89154-4002, USA*
[3]*Institute of Nuclear Science and Engineering, Idaho State University, 1776 Science Center Drive, Idaho Falls, Idaho 83401, USA*
[4]*University of Verona, Faculty of Mathematical, Physical and Natural Sciences, Ca'Vignal 2, Strada le Grazie 15, I-37134 Verona, Italy*
(Received 21 October 2007; revised manuscript received 29 December 2007; published 10 April 2008)

Synchrotron x-ray diffraction and diamond anvil cell techniques were used to characterize the phase transformations and to evaluate the structural stability at elevated pressures of a developed nanocrystalline composite. The optically transparent material was built of a germanium oxide-based amorphous host matrix with homogeneously dispersed 13 ± 3 nm Ga-Ge mullite-type nanocrystals, which had a structure similar to the conventional Al_2O_3-SiO_2 mullite. The equation of state of the nanocrystals and the overall structural integrity of the nanocomposite were investigated in quasihydrostatic conditions on compression to 36 GPa and on the following decompression to ambient conditions. The overall pressure-induced changes of x-ray diffraction patterns evidenced that the structural integrity of the material is well preserved up to about 14–16 GPa. The nanocomposite decompressed from 36 GPa to ambient pressure showed a very limited reversibility of the pressure-driven changes. A Birch-Murnaghan fit of the unit cell volume as a function of pressure yielded a zero-pressure bulk modulus, K_0, for the nanocrystalline phase of 229(15) GPa which makes this material potentially interesting for structural applications at elevated pressures.

DOI: 10.1103/PhysRevB.77.134107 PACS number(s): 62.50.−p, 61.46.−w, 61.05.cp, 64.30.−t

I. INTRODUCTION

In the search for novel functional materials one of the most promising avenues is the development of composites with nanometer-size structures or quantum dots dispersed in solid matrices. In particular, composites built of amorphous host matrices and high-density nanosized clusters of metallic, semiconductor, or dielectric type are attracting research attention due to their distinctive optical, electronic, thermal, or mechanical properties. Their numerous technological applications include zero-thermal expansion elements, very hard or architectural materials, bone implants, magnetic memory disk substrates, luminescent solar concentrators, or, in the telecom industry, active and passive optical devices.[1–4] Future applications of this type of nanocrystalline composites are likely to exploit highly specialized, on-demand engineered properties.

Beyond compositional changes and fabrication process modifications, an alternative way of adding new functionalities to materials in general and to nanocrystalline composites in particular is by exploiting high-pressure technology. Indeed, high pressure offers the opportunity to synthesize solids with unique optical, electronic, magnetic, or thermomechanical properties, which is currently a major challenge in materials science. Pressure-driven structural transformations in nanocrystalline composites are interesting from a fundamental science point of view, as well as are very attractive from the exciting prospect of fabricating novel materials.[5,6] As documented in our previous research, profound alterations in fundamental properties of nanocrystalline composites in response to elevated pressure could show a different way toward the development of technologically important materials.[7–9]

The nanocrystalline composite investigated in this study was derived from the GeO_2-Ga_2O_3-K_2O system. Our previous works on the microstructure of amorphous materials demonstrated that glasses belonging to GeO_2-Ga_2O_3-K_2O and GeO_2-Al_2O_3-K_2O systems are isostructural with SiO_2-Al_2O_3-K_2O glasses.[10,11] In the SiO_2-Al_2O_3 phase diagram, sillimanite, kyanite, and andalusite are high-pressure polymorphs of Al_2SiO_5 and mullite is the only stable crystalline phase under ambient pressure conditions.[12–15] The crystal structure of mullite is derived from that of sillimanite, with chains of AlO_6 octahedra cross-linked by (Si, Al) O_4 tetrahedra. Whereas sillimanite has silicon and aluminum cations ordered on the tetrahedral sites, mullite has excess Al^{3+} for Si^{4+}, with charge balance provided by oxygen vacancies. In other words, mullite has a defect sillimanite structure derived by $2Si^{4+}+O^{2-}=2Al^{3+}+O$ vacancy, with a typical oxygen vacancy of a few percent.[12–15] Typical mullites have a composition that usually lies between $3Al_2O_3 \cdot 2SiO_2$ and $2Al_2O_3 \cdot SiO_2$, and are one of the most promising engineering materials for structural and functional ceramics. Mullite ceramics, in addition to many conventional applications, were also proposed as matrix material for structural applications under extreme conditions[16,18] as well as candidates for window material in the mid-infrared range or as host media for several luminescent ions.[16,17]

In Ga_2O_3-GeO_2 and Al_2O_3-GeO_2 systems phases isostructural with Al-Si mullites were reported.[19–23] Al-Ge mul-

lites, in analogy to Al-Si mullites, have an extended stability range, but in different compositional domains. More specifically, where in the Al_2O_3-SiO_2 system at ambient pressure mullite is the only stable aluminosilicate formed, in the Al_2O_3-GeO_2 system two other stable compounds exist, namely, $Al_2Ge_2O_7$ and Al_2GeO_5.[19–21,23] Much less information is available for the Ga_2O_3-GeO_2 system where, besides mullite-type compounds such as Ga_2GeO_5, other crystalline phases—namely, $Ga_4Ge_3O_{12}$ and Ga_4GeO_8, with monoclinic unit cells and a very different stability range—were reported.[20,22,23]

In this paper, we report high-pressure investigations of a newly developed nanostructured composite, having Ga_2O_3-GeO_2 nanocrystals, structurally similar to Al_2O_3-SiO_2 mullite, and grown in an optically transparent amorphous host matrix. We use synchrotron x-ray diffraction and diamond anvil cell techniques to examine the structural integrity of this nanophased composite at elevated pressures. The results presented here are part of our extensive project on the development of optically transparent nanocomposites with specific nanostructures and tunable properties, based on dielectric matrices doped by nanocrystals.[7–9,24–29] With constantly increasing demand for "smarter" ceramics, these investigations provide not only a fundamental insight toward pressure-driven structural transformations, but also shed light on the possible practical applications of such nanocomposites.

II. EXPERIMENT

A number of nanocrystalline composites were synthesized starting from their amorphous precursors in a process involving high temperature melting, quenching, and successive isothermal treatments below glass transformation. The mixture for the glasses, which are the precursors of the composites, consisted of high-purity batch components and had a nominal composition represented by 5K:9Ga:23Ge:63O ratio in at. %. Details of the sample preparation have already been published elsewhere.[7,9,26,27] The development of distinct nanometer-size crystalline structures within the germanium oxide-based host matrix was thermally activated and modified in a controlled manner by the nucleation and growth conditions. Following this procedure several glass-ceramic nanocomposites were synthesized and one of them was selected for high-pressure investigations. High-resolution transmission electron microscopy (TEM) micrographs were taken with a Tecnai G2F30S-TWIN TEM microscope on a powdered sample spread over carbon-coated copper grids. The average diameter of the nanocrystals in the composite chosen for high-pressure studies was estimated to be 13 ± 3 nm. *In situ*, angle dispersive synchrotron x-ray diffraction studies were performed on compression to 36 GPa and successive decompression to ambient pressure. The powdered sample was compressed in a Mao-Bell-type diamond anvil cell (DAC) using diamonds with ~ 300 μm diameter culets. The sample chamber consisted of an ~ 120 μm diameter hole drilled in a rhenium gasket, preindented to a thickness of ~ 45 μm. A methanol-ethanol (4:1) mixture was used as a quasihydrostatic pressure-transmitting medium. A few grains of ruby powder were included and used to measure the pressure using the pressure scale of Mao *et al.*[30] The error in pressure for each pressure point was estimated from a few ruby chips scattered in the sample chamber. All high-pressure x-ray diffraction studies were performed at the 16-IDB undulator beamline of the High Pressure Collaborative Access Team (HPCAT), sector 16, Advanced Photon Source, Argonne National Laboratory, using a monochromatic synchrotron radiation source of 0.4245 Å. X-ray diffraction images were recorded using a MAR345 imaging plate as a detector and were next integrated and corrected for distortion using FIT2D software.[31] The sample-detector distance and geometric parameters were calibrated using a CeO_2 standard. The 10×10 μm^2 x-ray beam spot was achieved by microfocusing with two Kirckpatrick-Baez mirrors and a 30 μm diameter Mo cleanup pinhole to eliminate the beam tails. Indexing, least squares lattice parameter refinements and Rietveld full-profile structural refinements were done with the use of POWDER CELL[32] and TOPAS 2.1 (Bruker).[33] The average pattern acquisition time was 100 s. The time interval between each pressure increase (compression) or each pressure decrease (decompression) was about 15 min or less. Conventional angle dispersive x-ray diffraction patterns were collected in $\theta-2\theta$ Bragg-Brentano geometry, using a PANalytical X'Pert PRO X-ray diffractometer with Cu $K\alpha$ radiation (40 kV, 40 mA) and an X'Celerator solid state detector.

III. RESULTS

The building blocks of the optically transparent, nanocrystalline composite selected for high-pressure studies are (i) a germanium oxide-based host glass matrix, doped by potassium and (ii) homogeneously dispersed, mullite-type,[12–15] Ga_2O_3-GeO_2 nanocrystals of an average diameter 13 ± 3 nm. The resulting nanocrystalline Ga_2O_3-GeO_2 mullite will be hereafter referred to as nc-Ga-Ge mullite. Typical mullite such as $3Al_2O_3 \cdot 2SiO_2$ will be referred to as Al-Si mullite. Figure 1 shows a high-resolution transmission electron micrograph illustrating the microstructure of the nanocomposite, where the coherently scattering domains discernible within the amorphous host matrix indicate the presence of nanocrystals.

Figure 2 shows an ambient pressure x-ray diffraction pattern of the composite together with its Rietveld structural refinement. The unit cell of nc-Ga-Ge mullite belongs to the orthorhombic system, space group *Pbam* and Fig. 3 shows a model of the crystal lattice. The nucleated nanocrystals of nc-Ga-Ge mullite have a structure that is isomorphic with typical Al-Si mullites. The details of the structural refinement are presented in Sec. IV.

The pressure-induced evolution of the x-ray diffraction patterns was followed *in situ* (DAC) on compression to 36 GPa and on the consecutive decompression run to ambient pressure [Figs. 4(a) and 4(b)]. All diffraction patterns show Bragg lines of Ga-Ge mullite nanocrystals while the broad bands of background are due to the amorphous nature of the host matrix. With increasing pressure the diffraction lines of nc-Ga-Ge mullite shift toward higher 2θ angles. In compression above 16 GPa the lines of the nanocrystalline

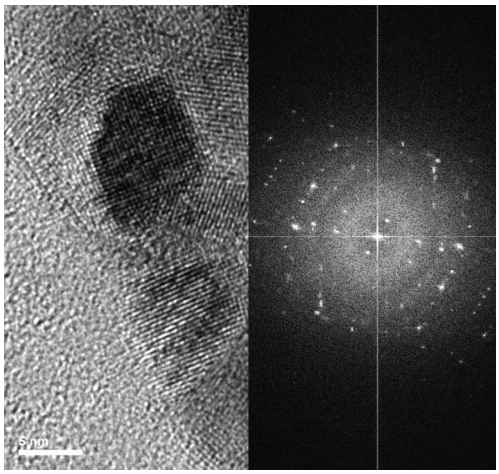

FIG. 1. Left: High-resolution transmission electron micrograph showing the structure of the nanocomposite: dark spots are nanocrystals embedded in the amorphous matrix. Right: selected area diffraction pattern illustrating the crystalline nature of the Ga-Ge mullite nanoparticles. The Ga-Ge mullite nanocrystals have a mean diameter of 13 ± 3 nm.

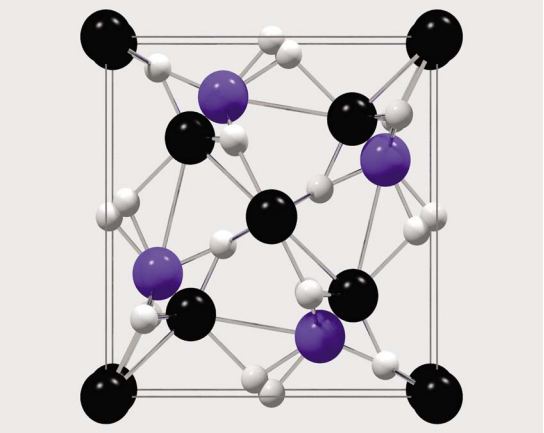

FIG. 3. (Color online) Model of the orthorhombic *Pbam* (S.G. 55, $Z=1$) crystal lattice of nc-Ga-Ge mullite. Black and white spheres represent Ga and O atoms, respectively. Blue spheres are at sites shared by Ga and Ge atoms. The lattice is shown in the *a*-*b* plane with the *c* axis being perpendicular to the plane of the page.

phase vanish and all the patterns are dominated by two very broad bands that increase in intensity and gradually shift to higher 2θ angles. The pattern of the nanocomposite quenched back to ambient pressure [Fig. 4(b)] did not show full reversibility of pressure-induced amorphization. However, as observed in the decompression run, the constant decrease of amorphous background intensity and the reemergence of small intensity peaks overlapped with the very broad amorphous bands, suggest that the pressure-induced amorphization of the nanocrystalline phase could be at least partially reversible [Figs. 4(b) and 7].

Rietveld structural refinements of the patterns of the compression run allowed us to evaluate the pressure-driven change of the unit cell of the nanocrystalline phase. In compression between ambient pressure and 16 GPa the unit cell density increased by 6.8% (Fig. 6). The most compressible lattice parameter was *c* with 4.2% compressibility comparing to 1.8% and 0.6% for *a* and *b* parameters, respectively (Fig. 5). The unit cell volume decreased by 6.5% and Fig. 6 illustrates the evolution of cell volume as a function of pressure.

IV. DISCUSSION

We report here the development of a distinctive type of nanocrystalline vitroceramic composite, with nucleated Ga-Ge mullite-type nanocrystals, dispersed in an amorphous host. A conventional angle-dispersive x-ray diffraction pattern of the nanocomposite selected for the high-pressure studies was used in order to refine the structure and to determine the unit cell parameters of the nanocrystalline phase at ambient pressure. Table I presents the results of structural refinements for both the nc-Ga-Ge mullite and, for comparison, for a typical Al-Si mullite.[12–15] A Rietveld refinement (Fig. 2) confirmed that in their ambient pressure and temperature form the nanocrystals nucleated in the host matrix have an orthorhombic crystal lattice with one formula unit per unit cell, belong to the space group *Pbam*, number 55, and have an estimated composition of $2.4Ga_2O_3 \cdot 1.9GeO_2$. The refined parameters of the unit cell are $a=7.8414(5)$ Å, $b=8.0193(5)$ Å, and $c=3.0031(2)$ Å, with cell volume of 188.84(2) $Å^3$ and density of 5.3572(6) g/cm^3 (Table I). Minor discrepancies between the observed and the calculated line intensities (Fig. 2) could be explained by a certain de-

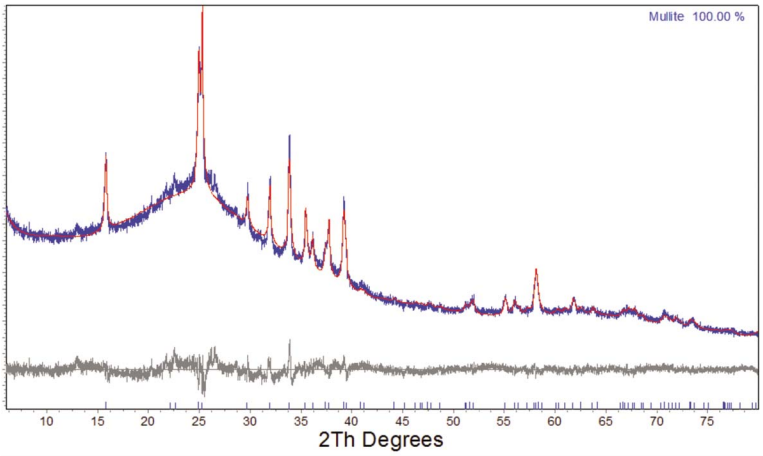

FIG. 2. (Color online) X-ray diffraction pattern and full-profile Rietveld structural refinement of nc-Ga-Ge mullite embedded in the germanium oxide-based amorphous host matrix of the nanocomposite. The fit has an $R_{wp}=1.8$ and the calculated intensities match well the observed intensities. Blue, red, and black solid lines represent experimental, calculated, and difference patterns, respectively. The pattern was collected in ambient pressure and temperature conditions using Cu $K\alpha$ radiation.

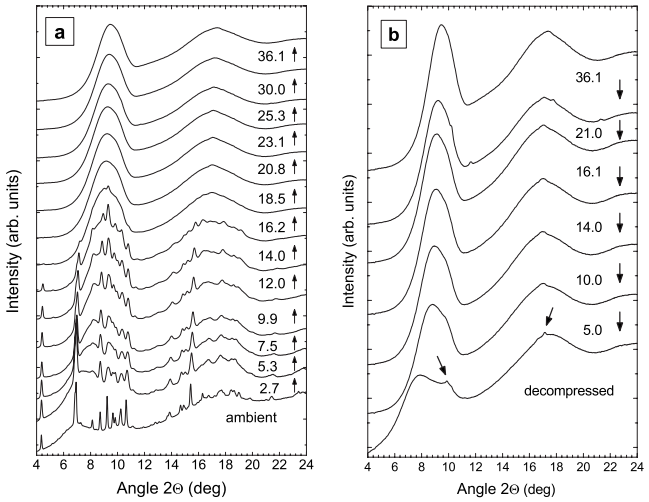

FIG. 4. [(a) and (b)] Selected angle-dispersive synchrotron x-ray diffraction patterns collected in the DAC: (a) in compression sequence to 36 GPa and (b) in the following decompression to ambient pressure. A mixture of methanol-ethanol (4:1) was used as a pressure-transmitting medium. The pressure-driven amorphization starts above 16 GPa. The arrows in the last decompression pattern mark the reappearance of the mentioned diffraction lines (small bands overlapping with the broad bands of the amorphous phase) suggesting a possible recovery, after pressure release, of the nanocrystalline phase.

gree of structural disorder and nonstoichiometry caused by oxygen vacancies, typical for this type of compounds. As can be seen in Table I, besides the fact that both mullite structures belong to an orthorhombic system (space group 55), they also have comparable atom positions. Considering the similarity of refinement results one can conceive that the nc-Ga-Ge mullite structure parallels that of Al-Si mullite, with Ga replacing Al atoms and with Ge replacing Si atoms. It is then rational to examine closer the structure of bulk

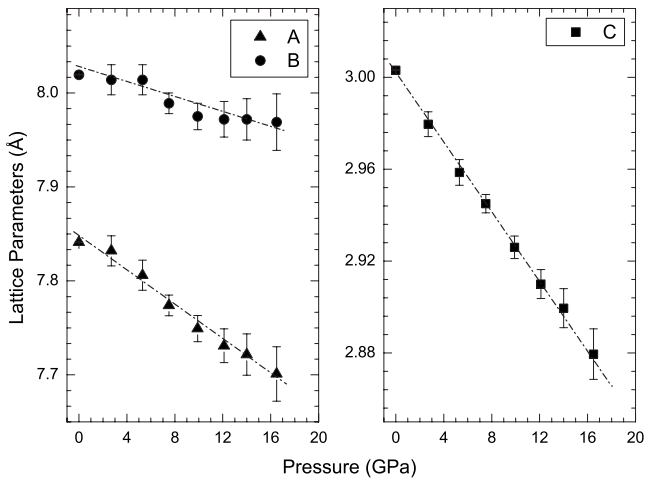

FIG. 5. Pressure-driven evolution of the unit cell parameters of the nc-Ga-Ge mullite: (left) *a* and *b* parameters; (right) *c* parameter. The most compressible lattice parameter was *c* with 4.2% compressibility comparing to 1.8% and 0.6% for *a* and *b* parameters, respectively. The dashed lines are drawn as a guide for the eyes.

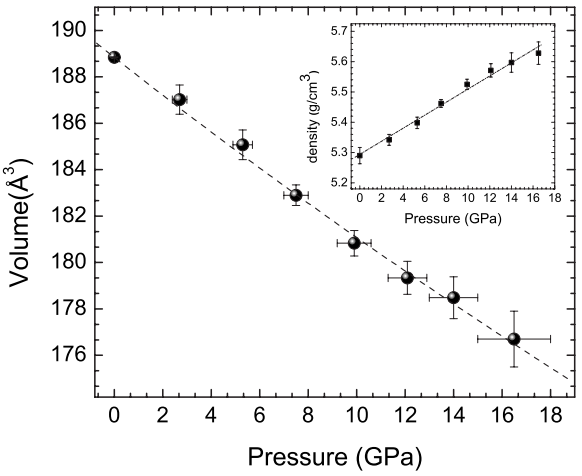

FIG. 6. Evolution of the unit cell volume of the nc-Ga-Ge mullite as a function of pressure increase. The estimated decrease of the cell volume for the compression run from ambient pressure up to 16 GPa is about 6.5%. The dashed line shows a Birch-Murnaghan fit of the experimental data. Inset: pressure-driven evolution of x-ray density of the nc-Ga-Ge mullite. The dashed lines are drawn as a guide for the eyes. The calculated density increase for the compression between ambient and 16.2 GPa is 6.8%.

Al-Si mullite, which has been thoroughly investigated in the literature, and make corresponding assumptions about the nanocrystalline Ga-Ge mullite structure. What is usually referred to as mullite in the Al_2O_3-SiO_2 system is a nonstoichiometric compound with composition described as a solid solution series of $Al_{4+2x}Si_{2-2x}O_{10-x}$, where x corresponds to the number of oxygen vacancies per unit cell.[12–15] Well ordered sillimanite Al_2SiO_5 corresponds to $x=0$ and mullite encompasses x ranging from about 0.18 to 0.82. The most frequently observed solid solutions are with $x=0.25$ and $x=0.40$, designated as 3:2-mullite ($3Al_2O_3 \cdot 2SiO_2$) and 2:1-mullite ($2Al_2O_3 \cdot SiO_2$), respectively.[12–15]

The estimated average composition of the nanocrystalline phase nucleated in the host matrix of the composite investigated here corresponds to $2.4Ga_2O_3 \cdot 1.9GeO_2$. This composition, though, is only a best approximation, since Ga and Ge atoms are not discernible by x rays, and we do not have in our possession the material in single crystal form; therefore, in Table I we report only an estimated distribution of atoms. The refinements demonstrated that, in analogy to bulk Al-Si mullite, our nc-Ga-Ge mullite has two partially occupied cation sites that are shared by the Ga^{3+} (instead of Al^{3+}) and Ge^{4+} (instead of Si^{4+}) ions (Table I). Al-Si mullite is built of edge-sharing AlO_6 octahedra, forming chains parallel to the *c* axis and cross-linked by tetrahedrally coordinated Si and Al, establishing double chains. Mullite has an excess of Al^{3+} for Si^{4+}, with charge balance provided by oxygen vacancies, typically 6–8%.[12–15] Likewise, in our nc-Ga-Ge mullite two of the four oxygen sites are only partially filled (Table I). In Al-Si mullite, besides the disorder on tetrahedral sites, where Al and Si atoms are randomly distributed, there is also an interstitial incorporation of some Al atoms. The same disorder probably occurs in the nc-Ga-Ge mullite. Considering the apparent similarity of nc-Ga-Ge mullite with Al-Si mullite the local structure of the mullite-type Ga-Ge nanocrystalline phase could be very complex.

TABLE I. Refined structural parameters of the ambient pressure nanocrystalline phase–nc-Ga-Ge mullite. The numbers in parentheses are the refined atom positions and for the unit cell parameters reflect standard deviations. The nucleated nanocrystals have a structure that is isomorphic with typical Al-Si mullites. Unit cell parameters for $3Al_2O_3 \cdot 2SiO_2$ mullite were taken from the ICSD database (No. 99330).

	$3Al_2O_3 \cdot 2SiO_2$ bulk mullite	$2.4Ga_2O_3 \cdot 1.9GeO_2$ nc-mullite
	Structure	
Space group	*Pbam*	*Pbam*
Z	1	1
	Lattice parameters	
a (Å)	7.5756(3)	7.84135(52)
b (Å)	7.6906(3)	8.01934(55)
c (Å)	2.8877(1)	3.00311(19)
Volume (Å^3)	168.24	188.843(21)
	Fractional coordinates (x,y,z)	
Al(1) or Ga(1)	(0, 0, 0)	(0, 0, 0)
Al(2) or Ga(2)	(0.1539, 0.3422, 0.5)	(0.1498, 0.3395, 0.5)
Si(1) or Ge(1)	(0.1539, 0.3422, 0.5)	(0.1498, 0.3395, 0.5)
Al(3) or Ga(3)	(0.2762, 0.2292, 0.5)	(0.2508, 0.2225, 0.5)
O(1)	(0.3538, 0.4212, 0.5)	(0.3507, 0.4212, 0.5)
O(2)	(0.1292, 0.2298, 0)	(0.1145, 0.2157, 0)
O(3)	(0.5, 0, 0.5)	(0.5, 0, 0.5)
O(4)	(0.4244, 0.0965, 0.5)	(0.4474, 0.0401, 0.5)

The evolution of x-ray diffraction patterns in compression to 36 GPa and in the following decompression runs to ambient conditions is shown in Figs. 4(a) and 4(b). The ambient pressure and the patterns below ~18 GPa are composed of two diffraction contributions, namely, broad bands of background due to the presence of the amorphous phase (host glass matrix) and the superimposed sharp diffraction lines of the nanocrystalline phase (nc-Ga-Ge mullite). The Bragg lines of nc-Ga-Ge mullite are still discernible in the 16.2 GPa pattern. All the patterns collected above this pressure contain two broad intense bands only, pointing toward a pressure-driven, temporary, or permanent amorphization of the nanocrystalline phase, the nc-Ga-Ge mullite. The overall pressure-induced changes of x-ray diffraction patterns suggest that the structural integrity of the material is well preserved up to 14 GPa and a loss of the material's structural integrity appears between 16 and 18 GPa. The Bragg lines' shift observed on compression [Fig. 4(a)] is associated with a gradually increasing line broadening which is a consequence of uniaxial stresses created by the diminishing hydrostatic conditions in the DAC.[34] The DAC is basically a uniaxial stress device and quasihydrostatic conditions are only obtained when the sample is contained within a fluid pressure medium.[35] When a methanol-ethanol mixture is employed as a pressure-transmitting medium, quasihydrostatic conditions are not preserved above ~10 GPa.

In the decompression run the reversibility of the pressure-induced amorphization of the nanocrystalline phase was

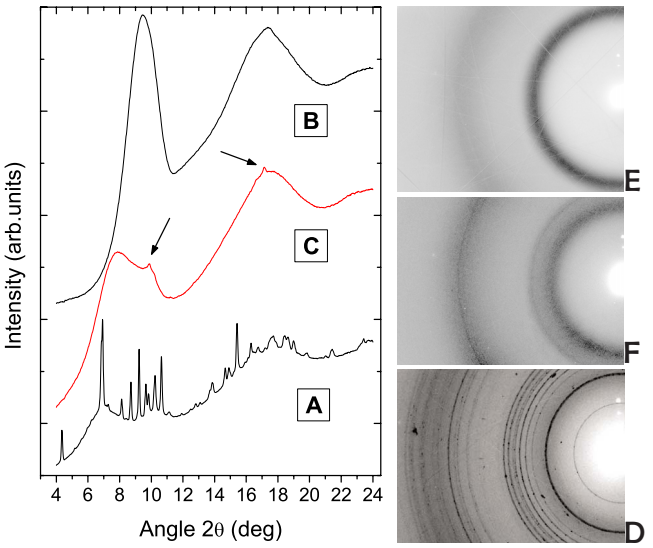

FIG. 7. (Color online) A comparison of synchrotron x-ray diffraction patterns (left) and corresponding diffractions images—powder diffraction rings (right) recorded using a MAR345 imaging plate as a detector: (A) beginning of compression (ambient pressure), (B) highest compression pressure 36 GPa, and (C) material decompressed back to ambient conditions. The arrows mark suggested reappearance of the diffraction lines suggesting possible recovery of nanocrystalline phase. Right: the corresponding pictures of the image plate showing powder diffraction rings, illustrating the progress of the phase transition: (D) ambient pressure, (E) at 36 GPa, and (F) decompressed to ambient pressure.

studied from 36 GPa down to ambient pressure [Fig. 4(b)]. The dominating broad diffraction bands of the amorphous phase decrease in intensity and shift toward lower 2θ angles. At the end of the decompression the bands reach almost their original position observed at the beginning of the compression run [Fig. 4(b)], indicating a progressive relaxation of the pressure-densified structure. A complete pressure release to ambient conditions suggests that the pressure-driven amorphization of the nanocrystalline phase is not entirely reversible under the experimental conditions applied and the high-pressure, amorphous phase is mostly retained on decompression. Even though the pressure-quenched nanocomposite does not show resolved Bragg lines of nanocrystals, the pattern demonstrates emerging small intensity bands, overlapped with the still dominating amorphous background [Figs. 4(b) and 7]. At this point, it is plausible to hypothesize that the decompressed material carries at least a signature or retains a memory of the initial ambient pressure phase, nc-Ga-Ge mullite. The same conclusion can be drawn from the comparison of the corresponding diffraction images that demonstrate the similarity of the ring structure of the pressure-quenched material to that observed at the beginning of the compression experiment (Fig. 7). In analogy to what happens with flexible structures exposed to elevated pressure, we may argue that in the compression mechanism the bond lengths and bond angles in the nanocrystals may temporarily vary without breaking of the bonds and may display x-ray detectable amorphization, comparable to a plastic deformation of the parent lattice.[8] If this is the case, then the

appearance (decompressed sample pattern) of the small intensity bands overlapped with dominating contribution of the amorphous background would indicate that after pressure release the decompressed structure still carries the signature of the initial nc-Ga-Ge mullite phase.

The literature reports few high-pressure studies of bulk, crystalline phases in the Al_2O_3-SiO_2 system. Al_2SiO_5 polymorphs (kyanite, andalusite, and sillimanite) were investigated up to about 20 GPa by static compression and up to 100 GPa by shock compression.[16,36] Static compression confirmed, at about 16 GPa, a pressure-induced disproportionation into a mixture of its component oxides, corundum, and stishovite.[16,36] The occurrence of disproportionation was also confirmed by *ab initio* calculations, based on density functional theory, for polymorphs of Al_2SiO_5 (kyanite, andalusite, sillimanite) and was explained in terms of classical crystal chemistry (Pauling's second rule).[37] For Al-Si mullite polycrystals shock compression studies were performed to 80 GPa to probe phase stability as well as the dynamic mechanical performance. The shock compression experiments yielded the Hugoniot elastic limit to be 16.1 ± 2.2 GPa, which is comparable to Al_2O_3, β-Si_3N_4, or SiC ceramics and is very high for an oxide.[38,39] This means that mullite-based ceramics with such a high value of dynamic compressive strength could offer a great potential as shock resistant materials. Furthermore, the Hugoniot data suggested that Al-Si mullite will undergo a pressure-induced phase transition at about 30 GPa that results in its disproportionation to corundum and stishovite with the presence of a mixed phase between 30 and 70 GPa. It was suggested that the disproportionation of mullite is very sluggish and of diffusive nature, with the high-pressure phase most likely amorphous due to insufficient time for the needed long range diffusion and ordering.[18] Based on the above discussion and considering the structural similarity of typical Al-Si mullite and the nc-Ga-Ge mullite in the studied nanocomposite we cannot exclude the possibility that our nanocrystalline mullite may perhaps also undergo pressure-driven disproportionation into rutile-like GeO_2 and the β-gallia elements. The planned, next run of high-pressure experiments involving some of the developed nanocomposites with various diameters of nanocrystals and additional experimental techniques is expected to shed more light on this matter.

Figure 6 shows the pressure dependence of the unit cell volume of nc-Ga-Ge mullite, calculated based on the lattice parameters obtained from the structural refinements. The pressure-driven cell volume decrease was 6.5% for the compression between ambient pressure and 16.5 GPa and it was accompanied by a cell density increase of 6.8% [Fig. 6 (inset)]. In order to determine the bulk modulus of the nanocrystalline phase K_0 and its pressure derivative K_0', the pressure-volume data were analyzed in terms of a third-order Birch-Murnaghan[40–42] equation of state (Fig. 6),

$$P = \frac{3}{2}K_0\left[\left(\frac{V_0}{V}\right)^{7/3} - \left(\frac{V_0}{V}\right)^{5/3}\right] \times \left\{1 + \frac{3}{4}(K_0' - 4)\left[\left(\frac{V_0}{V}\right)^{2/3} - 1\right]\right\}, \quad (1)$$

where V_0 is the volume at zero pressure, K_0 is the bulk modulus at zero pressure, and K_0' is its pressure derivative. The resulting zero-pressure bulk modulus K_0 and its pressure derivative K_0' for nc-Ga-Ge mullite at ambient conditions are $K_0 = 229(15)$ GPa and $K_0' = 2(0.9)$. This value of the bulk modulus is much higher than that reported in the literature ~174 GPa for bulk Al-Si mullite[18] and is not distant from that of the very hard corundum, α-Al_2O_3, ~257 GPa.[16] As was pointed out above, this value of the bulk modulus could be explained, to some extent, by the fact that the host glass matrix has a higher compressibility than the nanocrystals. Therefore the matrix can accommodate and relax the strains, which might otherwise be found at the surface of Ga-Ge mullite nanocrystals, hence preserving their structural integrity. Finally, the overall elastic properties of our glass-ceramic nanocomposite will also depend on the ratio of the crystalline-to-amorphous phase and on the diameter of the nanocrystalline phase.

In order to discuss the impact of pressure on the structure of the nanocrystalline phase of the studied composite, we have to keep in mind that the nanocrystals are embedded in the host glass matrix and in the most probable scenario the surrounding isotropic matrix distributes the impact of high pressure to the matrix-nanoparticle interface. The stability of a crystallite of a given size is determined by the relative importance of energy per unit volume, which favors crystal formation and energy per unit surface area of the opposite sign.[43,44] Crystallites of nanosized diameter scale have a large number of atoms within their surface area versus their volume. Consequently, the surface energy contributes substantially to the total energy of the crystallite. It was observed that when a phase transition in a bulk material is sharp, then in the corresponding nanocrystals it will be broad and will occur at higher pressures.[45,46] Among the four principal sources that could explain such behavior, including influence of host matrix, defects, quantum confinement effects, and surface tension, it was found that surface tension is the dominant factor in controlling the phase stability of nanocrystals embedded in a host matrix.[45–47] In addition, it has been shown that mechanical stability, hardness, melting point, sintering ability, electronic and magnetic structures, as well as compressibility are functions of particle diameter. Furthermore, for some materials, there is evidence that the bulk modulus and the equation of state also depend on crystallite size.[48,49] We studied here nanocrystals embedded in a glass host. What effect does the host have on the surface or interfacial tension? It was postulated that glasses at elevated pressure behave like elastic media and progressively transmit the pressure to the nanocrystalline phase.[7–9,45] In studies of nanometer-sized cadmium sulphate nanocrystals grown in a borosilicate glass it was found that they have very low interfacial tension and it was suggested that glass-embedded nanocrystals are inherently stable.[43] It was assumed that the glass matrix is able to accommodate and relax the strains that might otherwise be found at the surface of the nanoparticles, increasing their stability.[43] These and other findings[7–9,45] could contribute to explain the relatively high value of bulk modulus found for nc-Ga-Ge mullite and they hold promise for the potential practical applications of the composites with nanoparticles embedded in a glass.

V. CONCLUSIONS

We report here the development and synchrotron x-ray diffraction high-pressure studies of a distinct type of a nanocrystalline vitroceramic composite. The composite is built of nanometer-sized crystals of Ga-Ge mullite homogeneously dispersed in an amorphous host matrix built of germanium oxide doped by potassium. A Rietveld structural refinement confirmed that the nanocrystals belong to the space group *Pbam*, have a composition of $2.4Ga_2O_3 \cdot 1.9GeO_2$, and are structurally isomorphic with Al-Si mullite. Our study was designed to examine the overall structural integrity of the nanocomposite and to explore any pressure-induced structural modifications that may occur in nanocrystalline Ga-Ge mullite, at elevated pressures. Pressure-induced changes of x-ray diffraction patterns indicate that the structural integrity of the material is well preserved up to 14 GPa with a loss of integrity appearing around 16–18 GPa. The diffraction patterns of the nanocomposite gradually pressure-quenched to ambient conditions allow us to hypothesize that the structure of the decompressed nanocomposite retains a certain memory of the initial, ambient pressure structure of nc-Ga-Ge mullite. A Birch-Murnaghan equation of state yielded for nanocrystalline Ga-Ge mullite a zero-pressure bulk modulus, K_0 of 229(15) GPa, which is superior to that of bulk Al-Si mullite and not distant from that of corundum. Our studies allow us to conclude that this type of glass-derived nanocomposite, with tunable size of nanocrystals and high bulk modulus, could be very interesting for structural applications (matrix materials) under elevated pressure conditions.

ACKNOWLEDGMENTS

This work was performed at HPCAT (Sector 16), Advanced Photon Source (APS), Argonne National Laboratory. Use of the HPCAT Facility was supported by DOE-BES, DOE-NNSA (CDAC), NSF, DOD-TACOM, and the W. M. Keck Foundation. Use of the APS was supported by DOE-BES, under Contract No. DE-AC02-06CH11357. We are grateful to the HPCAT (Sector 16) staff, Advanced Photon Source (APS), Argonne National Laboratory for assistance in the setup.

*Author to whom correspondence should be addressed. lipinska@unlv.nevada.edu

[1] M. J. Dejneka, J. Non-Cryst. Solids **149**, 239 (1998).
[2] P. A. Tick, N. F. Borrelli, L. K. Cornelius, and M. A. Newhouse, J. Appl. Phys. **78**, 6367 (1995).
[3] Y. Wang and J. Ohwaki, Appl. Phys. Lett. **63**, 3268 (1993).
[4] G. H. Beall and L. R. Pinckney, J. Am. Ceram. Soc. **82**, 5 (1999).
[5] R. J. Hemley and N. W. Ashcroft, Phys. Today **51** (8), 26 (1998).
[6] R. J. Hemley, H. K. Mao, and V. V. Struzhkin, J. Synchrotron Radiat. **12**, 135 (2005).
[7] K. E. Lipinska-Kalita, B. Chen, M. B. Kruger, Y. Ohki, J. Murowchick, and E. P. Gogol, Phys. Rev. B **68**, 035209 (2003).
[8] K. E. Lipinska-Kalita, G. Mariotto, P. E. Kalita, and Y. Ohki, Physica B **365**, 155 (2005).
[9] K. E. Lipinska-Kalita, S. A. Gramsch, P. E. Kalita, and R. J. Hemley, J. Raman Spectrosc. **36**, 938 (2005).
[10] K. E. Lipinska-Kalita and D. J. Mowbray, J. Non-Cryst. Solids **122**, 1 (1990).
[11] K. E. Lipinska-Kalita and G. Mariotto, J. Non-Cryst. Solids **128**, 285 (1991).
[12] R. J. Angel and C. T. Prewitt, Am. Mineral. **71**, 1476 (1986).
[13] P. Rehak, G. Kunath-Fandrei, P. Losso, B. Hildmann, H. Schneider, and C. Jäger, Am. Mineral. **83**, 1266 (1998).
[14] D. Voll, C. Lengauer, A. Beran, and H. Schneider, Eur. J. Mineral. **13**, 591 (2001).
[15] D. J. Lacks, B. Hildmann, and H. Schneider, Phys. Rev. B **72**, 214305 (2005).
[16] N. Kawai, K. G. Nakamura, and K. Kondo, J. Appl. Phys. **96**, 4126 (2004).
[17] A. Aksay, D. M. Dabbs, and M. Savikaya, J. Am. Ceram. Soc. **74**, 2343 (1991).
[18] U. Steinhauser, W. Braue, J. Götring, B. Kanka, and H. Schneider, J. Eur. Ceram. Soc. **20**, 651 (2000).
[19] A. Kahn-Harari, S. Abolhassani, J. G. Perez-Ramirez, D. Michel, L. Mazerolles, R. Portier, and G. J. Perez-Ramirez, J. Solid State Chem. **90**, 23448 (1991).
[20] D. Michel, Ph. Colomban, S. Abolhassani, F. Voyrorf, and A. Kahn-Harari, J. Eur. Ceram. Soc. **16**, 161 (1996).
[21] H. Ledbetter, S. Kim, D. Balzar, S. Crudele, and W. Kriven, J. Am. Ceram. Soc. **81**, 1025 (1998).
[22] A. Kahn, A. Agafonov, D. Michel, and M. Perez Jorba, J. Solid State Chem. **65**, 377 (1986).
[23] M. D. Colomban, P. Abolhassani, S. Voyron, and F. Kahn-Harari, J. Eur. Ceram. Soc. **16**, 161 (1996).
[24] F. Auzel, K. E. Lipinska-Kalita, and P. Santa-Cruz, Opt. Mater. (Amsterdam, Neth.) **5**, 75 (1996).
[25] R. Ceccato, R. Dal Maschio, G. Mariotto, M. Montagna, F. Rossi, M. Ferrari, K. E. Lipinska-Kalita, and Y. Ohki, J. Appl. Phys. **90**, 2522 (2001).
[26] K. E. Lipinska-Kalita, D. M. Krol, R. J. Hemley, P. E. Kalita, C. L. Gobin, and Y. Ohki, J. Appl. Phys. **98**, 054302 (2005).
[27] K. E. Lipinska-Kalita, D. M. Krol, R. J. Hemley, G. Mariotto, P. E. Kalita, and Y. Ohki, J. Appl. Phys. **98**, 054301 (2005).
[28] K. E. Lipinska-Kalita, D. M. Krol, R. J. Hemley, P. E. Kalita, C. L. Gobin, and Y. Ohki, J. Non-Cryst. Solids **352**, 524 (2006).
[29] K. E. Lipinska-Kalita, P. Kalita, O. Hemmers, C. Gobin, G. Mariotto, T. Hartmann, and L. Ma, Bull. Am. Phys. Soc. **52** (2007), http://meetings.aps.org/link/BAPS.2007.MAR.D43.13
[30] H. K. Mao, P. M. Bell, J. W. Shaner, and D. J. Steinberg, J. Appl. Phys. **49**, 3276 (1978).
[31] A. P. Hammersley, FIT2D V10.3, V4.0 ESRF, Grenoble, 1998.
[32] W. Kraus and G. Nolze, POWDER CELL 2.4, FIMRT, Berlin, 2004.
[33] DiffracPlus TOPAS 2.1, Bruker AXS, 2006.
[34] M. Gauthier, High Press. Res. **22**, 779 (2002).
[35] A. Jayaraman, Rev. Mod. Phys. **55**, 65 (1983).
[36] M. W. Schmidt, S. Poli, P. Comodi, and P. F. Zanazzi, Am. Mineral. **82**, 460 (1997).

[37] A. R. Oganov and J. P. Brodholt, Phys. Chem. Miner. **27**, 430 (2000).
[38] H. He, T. Sekine, T. Kobayashi, H. Hirosaki, and I. Suzuki, Phys. Rev. B **62**, 11412 (2000).
[39] T. Sekine and T. Kobayashi, Phys. Rev. B **55**, 8034 (1997).
[40] F. D. Murnaghan, Am. J. Math. **49**, 235 (1937).
[41] F. Birch, Phys. Rev. **71**, 809 (1947).
[42] F. Birch, J. Geophys. Res. B **83**, 1257 (1978).
[43] T. M. Hayes, L. B. Lurio, J. Pant, and P. D. Persans, Phys. Rev. B **63**, 155417 (2001).
[44] P. D. Persans, L. B. Lurio, J. Pant, H. Yukselici, G. Lian, and T. M. Hayes, J. Appl. Phys. **87**, 3850 (2000).
[45] M. R. Silvestri and J. Schroeder, J. Phys.: Condens. Matter **7**, 8519 (1995).
[46] C. C. Chen, A. B. Herhold, C. S. Johnson, and A. P. Alivisatos, Science **276**, 398 (1997).
[47] J. N. Wickham, A. B. Herhold, and A. P. Alivisatos, Phys. Rev. Lett. **84**, 923 (2000).
[48] S. H. Tolbert, A. B. Herhold, C. S. Johnson, and A. P. Alivisatos, Phys. Rev. Lett. **73**, 3266 (1994).
[49] S. H. Tolbert and A. P. Alivisatos, J. Chem. Phys. **102**, 4642 (1995).